



International Carbon Conference 2018, ICC 2018, 10–14 September 2018, Reykjavik, Iceland

The chemistry and potential reactivity of the CO₂-H₂S charged injected waters at the basaltic CarbFix2 site, Iceland

Deirdre E. Clark^{a,*}, Ingvi Gunnarsson^b, Edda S. Aradóttir^b, Magnús Þ. Arnarson^c,
Þorsteinn A. Þorgeirsson^b, Sigrún S. Sigurðardóttir^b, Bergur Sigfússon^b,
Sandra Ó. Snæbjörnsdóttir^b, Eric H. Oelkers^d, and Sigurður R. Gíslason^a

^a*Institute of Earth Sciences, University of Iceland, Sturlugata 7, 101 Reykjavík, Iceland*

^b*Reykjavík Energy, Bæjarhálsi 1, 110 Reykjavík, Iceland*

^c*Orka náttúrunnar, Bæjarhálsi 1, 110 Reykjavík, Iceland*

^d*GET, CNRS/UMR5563, 14 Avenue Edouard Belin, 31400 Toulouse, France*

Abstract

The CarbFix2 project aims to capture and store the CO₂ and H₂S emissions from the Hellisheiði geothermal power plant in Iceland by underground mineral storage. The gas mixture is captured directly by its dissolution into water at elevated pressure. This fluid is then injected, along with effluent geothermal water, into subsurface basalts to mineralize the dissolved acid gases as carbonates and sulfides. Sampled effluent and gas-charged injection waters were analyzed and their mixing geochemically modeled using PHREEQC. Results suggest that carbonates, sulfides, and other secondary minerals would only precipitate after it has substantially reacted with the host basalt. Moreover, the fluid is undersaturated with respect to the most common primary and secondary minerals at the injection well outlet, suggesting that the risk of clogging fluid flow paths near the injection well is limited.

Copyright © 2018 Elsevier Ltd. All rights reserved.

Selection and peer-review under responsibility of the publication committee of the International Carbon Conference 2018.

Keywords: CO₂ sequestration; H₂S sequestration; gas injection; mineral storage; CCS, basalt

1. Introduction

Reykjavik Energy, the largest geothermal power company in Iceland, alongside the CarbFix group has developed a pioneering method to capture their carbon dioxide (CO₂) and hydrogen sulfide (H₂S) emissions and store as minerals

* Corresponding author. Tel.: +354-525-4274

E-mail address: dec2@hi.is

in subsurface basalts. The emission of these geothermal gases in addition to hydrogen (H_2), nitrogen (N_2), methane (CH_4), and argon (Ar) are associated with high-temperature geothermal systems.

Carbon capture and storage is one solution to reduce CO_2 emissions into the atmosphere. This approach was successfully tested as a part of the original CarbFix CO_2 storage project at the Hellisheiði Geothermal Power Plant in Iceland. Basaltic rocks, like those found at Hellisheiði, are rich in divalent cations, Ca^{+2} , Mg^{+2} , and Fe^{+2} , which react with CO_2 dissolved in water to form stable carbonate minerals. Results from field injections at the original CarbFix low temperature site (20 – 50 °C) showed mineralization of injected dissolved acid gases had occurred in less than two years [1-3].

The efforts on H_2S sequestration followed a regulation passed by the Government of Iceland in 2010 restricting atmospheric H_2S emissions. This ruling required the geothermal industry in Iceland, locally the largest anthropogenic source of sulfur, to significantly reduce their emissions [4-6]. H_2S abatement by sulfur mineral storage was proposed by Stefánsson et al. [7] and preliminary efforts were made through gas capture and injection tests in 2012 [4, 8].

These initial pilot studies were upscaled starting in June 2014 as part of the CarbFix2 project, where a mixture of CO_2 and H_2S was co-injected with effluent geothermal water from the power plant to a depth of 750 m with temperatures of 240 – 250 °C [9]. By the end of 2017, 23,104 tons of CO_2 and 11,853 tons of H_2S had been injected, accounting for approximately 34% of the CO_2 and 68% of the H_2S 2017 emissions of the Hellisheiði power plant. Once in the geothermal reservoir, heat exchange and host rock dissolution neutralizes the gas-charged water and saturates the injected fluid with respect to carbonate and sulfur minerals.

To better characterize the long-term behavior of the CarbFix2 acid gas storage effort, specifically the conditions within the injection wells, both the gas-charged and effluent waters were sampled from the head of the injection wells. The mixing of these two waters at more than 750 m depth was geochemically modeled using PHREEQC to calculate the changes in pH, temperature and fluid composition. The stability of the primary and secondary minerals at the injection well outlet was also assessed as the fluids mixed and heated up in the high temperature geothermal reservoir.

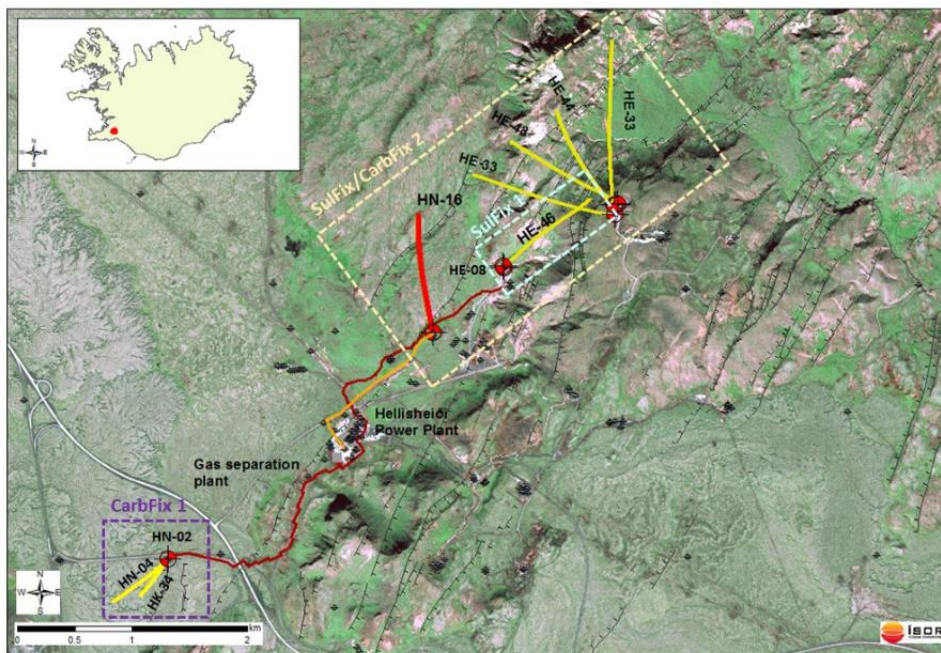


Fig.1 Aerial map of the original CarbFix and the CarbFix2 injection sites and the HN-16 injection well (shown in bright red). Taken from Aradóttir et al. [4].

Table 1. Dissolution reactions

Gas	Reactions
CO ₂	$\text{CO}_{2(\text{g})} + \text{H}_2\text{O} = \text{H}_2\text{CO}_3$
	$\text{H}_2\text{CO}_3 = \text{HCO}_3^- + \text{H}^+$
	$\text{HCO}_3^- = \text{CO}_3^{2-} + \text{H}^+$
H ₂ S	$\text{H}_{2\text{S}(\text{g})} = \text{H}_{2\text{S}(\text{aq})}$
	$\text{H}_{2\text{S}(\text{aq})} = \text{HS}^- + \text{H}^+$
	$\text{HS}^- = \text{S}^{2-} + \text{H}^+$

2. Materials and Methods

2.1. Capture and injection

The CarbFix2 injection site is located adjacent to the Hellisheiði Geothermal Power Plant, 25 km east of Reykjavík, Iceland (Fig. 1). The Hellisheiði geothermal field is a part of the southern Hengill volcanic system, which consists of fractured, hydrothermally altered basalts. Further details describing the geology of the site are reported by Gunnarsson et al. [9] and Franzson et al. [10-11].

About 40,000 tonnes of CO₂ and 9,000 tonnes of H₂S are produced out of the geothermal reservoir annually along with a minor amount of H₂, N₂, Ar, and CH₄. A scrubbing tower was used to dissolve a CO₂ and H₂S dominated gas mixture under anoxic conditions from the exhaust gas stream into pure water (condensate), in accord with the reactions shown in Table 1. This method allows for immediate solubility trapping with the added security of no potential gas leaks during the injection of this fluid into the subsurface [4,9]. Note that the dissolution of these gases liberate H⁺ leading the gas-charged fluids to become acidic and thus reactive when in contact with basalts.

Starting in June 2014, approximately 25% of the exhaust gas from the power plant was processed through the scrubbing tower that operated at a pressure of 5 bars. Flow rates were optimized to recover 56% of the CO₂ and 97% of the H₂S from the exhaust stream. The gas-charged condensate water at a temperature of 20 °C was then pressurized to 9 bars and transported 1.5 km to the injection well HN-16 (Fig. 1), where it was subsequently injected into the subsurface at a rate of 30 to 36 kg/s together with a known flux of effluent water [9]. From 16 July 2016 the scrubbing tower gas capture capacity was doubled and operated at 6 bars before being transported to HN-16 and co-injected with the effluent water. This change in capture rate altered somewhat the composition of the injected gas-charged fluid. In addition, starting at this time, a minor quantity of the acid gases was added to the effluent water to prevent pipe clogging. Prior to the addition of the acid gases, the effluent geothermal water had an average pH of 9.13, but after it was 7.5. As such two sets of geochemical measurements are presented, one for the average compositions of the fluids before and one for after July 2016 (Table 2). The co-injected effluent water had a temperature ranging from 55 to 140 °C and was injected at a rate of 10 to 130 kg/s.

These fluids were injected into the HN-16 injection well. HN-16 was directionally drilled, 2206 m long and 0.311 m wide, with the top 660 m encased in carbon steel. The two fluids (acid gas-charged condensate and effluent geothermal water) were injected separately to a depth of 700 m (Fig. 2), where they then mixed and flowed into the main target aquifer at a depth between 1900 and 2200 m and a temperature range from 220 to 260 °C [9]. Table 3 lists the primary and secondary minerals expected to be present within this aquifer, together with their dissolution reactions [12].

Table 2. Average geochemical compositions of injected effluent geothermal and gas-charged waters before and after July 2016. Average concentrations reported for the first injection scenario (June 2014 – July 2016) are taken from Gunnarsson et al. [9]. Values given in mmol/kg.

Injection Scenario		June 2014 – July 2016 ¹⁹⁾	July 2016 – Dec 2017
Gas-charged water	pH	3.65	3.54
	DIC	102	101
	H ₂ S	72.9	166
Effluent water	pH	9.13	7.5
	DIC	0.424	1.53
	H ₂ S	0.442	1.21
	SO ₄	0.246 ^a	0.110 ^b
	Si ^c	8.17	7.88
	Na ^c	6.13	5.65
	K ^c	0.616	0.600
	Ca ^c	0.0143	0.0101
	Mg ^c	< 0.002	0.003
	Fe	< 0.001 ^c	0.0005 ^d
	Al ^c	0.047	0.041
	Cl	3.36 ^a	3.66 ^b
	F	0.051 ^a	0.049 ^b

^aMeasured by ICS-1100

^bMeasured by ICS-2000

^cMeasured by ICP-OES

^dMeasured by ICP-MS

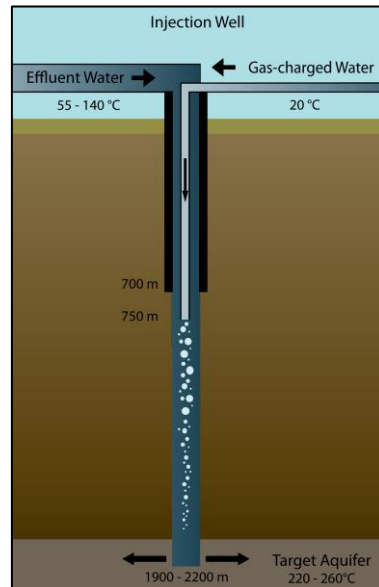


Fig. 2. Schematic diagram of the injection system, from the fluid inlets at the well head to the outlet within the reservoir. Within the casing of each well is a 4" stainless steel pipe that reaches 750 m, thus preventing any contact between the carbon steel and the gas-charged water. The two fluids, effluent water and gas-charged water, were injected separately, mixing at the exit of the stainless steel pipe. The main aquifer receiving the water mixture was located at a depth between 1900 and 2200 m with a temperature of 220 – 260 °C.

Table 3. Dissolution reactions of primary and secondary minerals present in the target basaltic reservoir.

Minerals	Dissolution reaction	
Primary	Basalt	$\text{SiAl}_{0.35}\text{O}_2(\text{OH})_{1.05} + 1.05 \text{ H}^+ = 0.35 \text{ Al}^{+3} + \text{SiO}_2 + 1.05 \text{ H}_2\text{O}$
	Albite	$\text{NaAlSi}_3\text{O}_8 + 4 \text{ H}^+ = \text{Al}^{+3} + \text{Na}^+ + 3 \text{ SiO}_2 + 2 \text{ H}_2\text{O}$
	Anorthite	$\text{CaAl}_2\text{Si}_2\text{O}_8 + 8 \text{ H}^+ = \text{Ca}^{+2} + 2 \text{ Al}^{+3} + 2 \text{ SiO}_2 + 4 \text{ H}_2\text{O}$
	Diopside	$\text{CaMgSi}_2\text{O}_6 + 4 \text{ H}^+ = \text{Ca}^{+2} + \text{Mg}^{+2} + 2 \text{ SiO}_2 + 2 \text{ H}_2\text{O}$
	Enstatite	$\text{MgSiO}_3 + 2 \text{ H}^+ = \text{Mg}^{+2} + \text{SiO}_2 + \text{H}_2\text{O}$
	Fayalite	$\text{Fe}_2\text{SiO}_4 + 4 \text{ H}^+ = 2 \text{ Fe}^{+2} + \text{SiO}_2 + 2 \text{ H}_2\text{O}$
	Ferrosilite	$\text{FeSiO}_3 + 2 \text{ H}^+ = \text{Fe}^{+2} + \text{SiO}_2 + \text{H}_2\text{O}$
	Forsterite	$\text{Mg}_2\text{SiO}_4 + 4 \text{ H}^+ = 2 \text{ Mg}^{+2} + \text{SiO}_2 + \text{H}_2\text{O}$
	Magnetite	$\text{Fe}_3\text{O}_4 + 8 \text{ H}^+ = \text{Fe}^{+2} + 2 \text{ Fe}^{+3} + 4 \text{ H}_2\text{O}$
Secondary	Calcite	$\text{CaCO}_3 + \text{H}^+ = \text{Ca}^{+2} + \text{HCO}_3^-$
	Clinocllore	$\text{Mg}_5\text{Al}_2\text{Si}_3\text{O}_{10}(\text{OH})_8 + 16 \text{ H}^+ = 5 \text{ Mg}^{+2} + 2 \text{ Al}^{+3} + 3 \text{ SiO}_2 + 12 \text{ H}_2\text{O}$
	Daphnite	$\text{Fe}_5\text{Al}_2\text{Si}_3\text{O}_{10}(\text{OH})_8 + 16 \text{ H}^+ = 5 \text{ Fe}^{+2} + 2 \text{ Al}^{+3} + 3 \text{ SiO}_2 + 12 \text{ H}_2\text{O}$
	Epidote	$\text{Ca}_2\text{FeAl}_2\text{Si}_3\text{O}_{12}(\text{OH}) + 13 \text{ H}^+ = 2 \text{ Ca}^{+2} + \text{Fe}^{+2} + 2 \text{ Al}^{+3} + 3 \text{ SiO}_2 + 7 \text{ H}_2\text{O}$
	Ferroactinolite	$\text{Ca}_2\text{Fe}_5\text{Si}_8\text{O}_{22}(\text{OH})_2 + 14 \text{ H}^+ = 2 \text{ Ca}^{+2} + 5 \text{ Fe}^{+2} + 8 \text{ SiO}_2 + 8 \text{ H}_2\text{O}$
	Prehnite	$\text{Ca}_2\text{Al}_2\text{Si}_3\text{O}_{10}(\text{OH})_2 + 10 \text{ H}^+ = \text{Ca}^{+2} + 2\text{Al}^{+3} + 3 \text{ SiO}_2 + 6 \text{ H}_2\text{O}$
	Pyrite	$\text{FeS}_2 + \text{H}_2\text{O} = \text{Fe}^{+2} + 0.25 \text{ H}^+ + 0.25 \text{ SO}_4^{-2} + 1.75 \text{ HS}^-$
	Pyrrhotite	$\text{FeS} + \text{H}^+ = \text{Fe}^{+2} + \text{HS}^-$
	Tremolite	$\text{Ca}_2\text{Mg}_5\text{Si}_8\text{O}_{22}(\text{OH})_2 + 14 \text{ H}^+ = 2 \text{ Ca}^{+2} + 5 \text{ Mg}^{+2} + 8 \text{ SiO}_2 + 8 \text{ H}_2\text{O}$
	Wairakite	$\text{CaAl}_2\text{Si}_4\text{O}_{10}(\text{OH})_4 + 8 \text{ H}^+ = \text{Ca}^{+2} + 2 \text{ Al}^{+3} + 4 \text{ SiO}_2 + 6 \text{ H}_2\text{O}$
	Wollastonite	$\text{CaSiO}_3 + 2 \text{ H}^+ = \text{Ca}^{+2} + \text{SiO}_2 + \text{H}_2\text{O}$

2.2. Sampling and analysis

The effluent and gas-charged waters were sampled at the HN-16 injection well. The dissolved inorganic carbon (DIC) and H_2S concentrations in the gas-charged pure water were determined from collected water samples. The effluent water samples were analyzed for DIC, H_2S , and SO_4^{-2} . The sampling and analysis methods are described by Gunnarsson et al. [9]. Major elements of the effluent water were also measured either by Ion Chromatography (Dionex ICS-1100 or ICS-2000 chromatography system), Inductively Coupled Plasma Optical Emission Spectrometer (ICP-OES), or Inductively Coupled Plasma Mass Spectrometer (ICP-MS). Fluids were acidified with concentrated supra-pure HNO_3 (1.0 vol %) prior to analysis by ICP-OES and ICP-MS while no preparation was required for IC analysis. Analytical uncertainties of these analyses were on the order of $\leq 5\%$.

2.3. Modeling

The goal of the modeling is to determine the potential for secondary minerals to form in and near the well prior to substantial dissolution of the host rock. The geochemical speciation program PHREEQC 3.4.0 was used together with its *core10.dat* database and additional modifications [13–15] to determine the pH, temperature and geochemical speciation of the injection mixture in addition to the saturation index of the primary and secondary minerals expected to be present or potentially forming during the injection. The saturation index is defined as $\text{SI} \equiv \log_{10} \Omega$; saturation state, Ω , is calculated from $\Omega \equiv Q/K_{\text{SP}}$, where K_{SP} is the equilibrium constant of the mineral dissolution reaction, and Q is the corresponding reaction quotient of a specific solution. A solution is oversaturated with a mineral if a saturation index is greater than zero and undersaturated if less than zero.

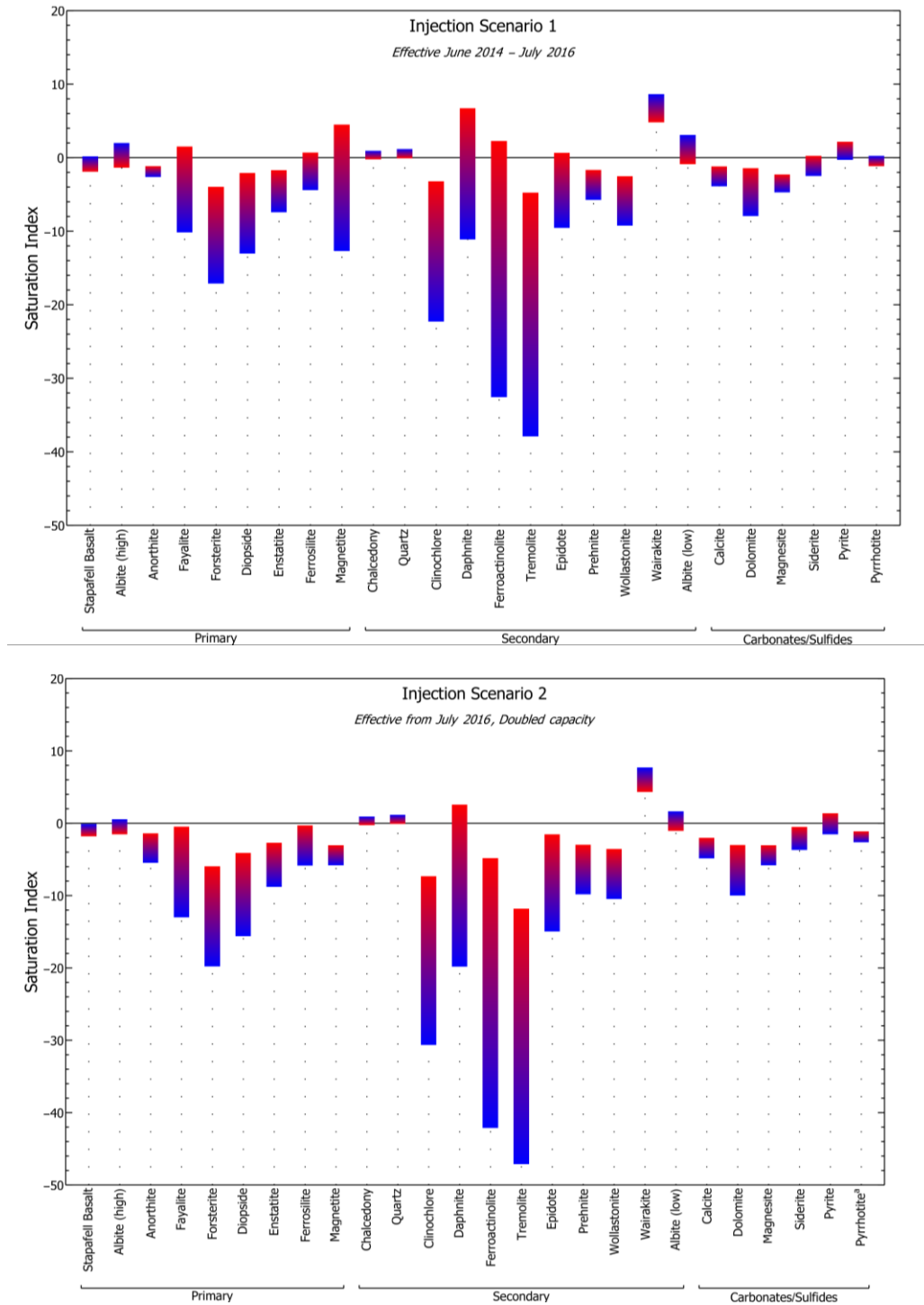


Fig. 3. The calculated saturation index of primary and secondary minerals during Injection Scenario 1 (top) and 2 (bottom) over a temperature range of 60 to 260 °C, which occurs as the injected fluids heat within and close to the injection wells. The coolest temperature is represented by blue and the warmest by red. Note that these waters reflect a starting effluent water temperature of 80 °C.

*The saturation state of pyrrhotite during Scenario 2 does not increase continuously with temperature; it is closest to saturation at 150 °C.

The average DIC, H₂S, and major element concentrations of the measured gas-charged and effluent water were adopted to model the chemistry of the mixed injection fluid. The original temperature of the gas-charged water was 20 °C, whereas that of the effluent water ranged from 55 to 140 °C. The resulting mixed fluid was heated to 260 °C during its descent in the well and its arrival into the main target reservoir. Hence, mineral saturation states of the gas-charged and effluent water mixture have been modeled as a function of temperature. No dissolution or precipitation was allowed to occur during the simulation. The fluid pressure was fixed at 81.6 bars to reflect that of the target reservoir.

3. Results

The average DIC, H₂S, and major element concentrations of the gas-charged and effluent water are reported in Table 2. Values from the June 2014 – July 2016 injection period are averaged from results in Gunnarsson et al. [9].

Changes in the calculated pH and temperature of the injection fluids having different mixing ratios of the effluent and gas-charged waters were calculated. Saturation state results are presented in Fig. 3 for the target fluid mixing ratio of 30% gas-charged condensate and 70% effluent water and an initial fluid temperature mixture of 80 °C. The pH of the mixed injection fluids were 5.4 and 4.7, respectively, for the fluid mixture before and after July 2016.

For both sets of fluid compositions, the fluids were considerably undersaturated with the most potential secondary phases at the maximum modeled temperature of 260 °C (Fig. 3). Siderite was the only carbonate close to saturation at the highest temperatures, whereas the remaining CO₂-bearing minerals were undersaturated at all temperatures. Pyrite was at saturation and pyrrhotite below. Daphnite, the Fe endmember of chlorite, became supersaturated; ferroactinolite, the Fe endmember of actinolite, also showed a similar pattern, although in the second scenario it did not reach saturation.

4. Discussion and Conclusions

The findings summarized above suggest that little to no mineral precipitation would be expected to occur from the fluids injected into the CarbFix2 storage site during its descent within the injection wells and immediately following its release to the main basaltic target reservoir. The major reactions will be the dissolution of the host basalt in the vicinity of the well, thereby increasing the rock permeability. Any secondary minerals expected to precipitate would do so only after a significant volume of basalt has been dissolved into the injected fluids as they move away from the injection point. These results therefore suggest that there is minimal risk to clog injection wells and the pore space close to the wells. Furthermore, doubling the CO₂ and H₂S injection rates and adding gas to the effluent water before injection lowers the saturation state of most primary and secondary minerals within and adjacent to the injection wells.

Acknowledgements

This publication has been produced with support from Reykjavik Energy and the European Commission through the projects CarbFix (EC coordinated action 283148) and CO₂-REACT (EC Project 317235). Special thanks to Martin Voigt for his help and support.

References

- [1] Matter J.M., M. Stute, S.Ó. Snæbjörnsdóttir, E.H. Oelkers, S.R. Gíslason, E.S.P. Aradóttir, B. Sigfússon, I. Gunnarsson, H. Sigurdardóttir, E. Gunnlaugsson, G. Axelsson, H.A. Alfredsson, D. Wolff-Boenisch, K. Mesfin, D. Fernandez de la Reguera Taya, J. Hall, K. Dideriksen, and W.S. Broecker. "Rapid carbon mineralization for permanent disposal of anthropogenic carbon dioxide emissions" *Science* 352 (2016): 1312-1314.
- [2] Snæbjörnsdóttir S.Ó., E.H. Oelkers, K. Mesfin, E.S.P. Aradóttir, K. Dideriksen, I. Gunnarsson, E. Gunnlaugsson, J.M. Matter, M. Stute, and S.R. Gíslason. "The chemistry and saturation states of subsurface fluids during the in-situ mineralization of CO₂ and H₂S at the CarbFix site in SW-Iceland" *International Journal of Greenhouse Gas Control* 58 (2017): 87-102.
- [3] Gíslason S.R., and E.H. Oelkers. "Carbon Storage in Basalt" *Science* 344 (2014): 373-374.

- [4] Aradóttir E.S., I. Gunnarsson, B. Sigfússon, S.R. Gíslason, E.H. Oelkers, M. Stute, J.M. Matter, S.Ó. Snæbjörnsdóttir, K. Mesfin, H.A. Alfredsson, J. Hall, M.Th. Arnarsson, K. Dideriksen, B.M. Júlíusson, W.S. Boecker, and E. Gunnlaugsson. “Towards Cleaner Geothermal Energy: Subsurface Sequestration of Sour Gas Emissions from Geothermal Power Plants” *World Geothermal Congress*, Melbourne, Australia (2015).
- [5] Júlíusson B.M., I. Gunnarsson, K.V. Matthíasdóttir, S.M. Markússon, B. Bjarnason, Ó.G. Sveinsson, Th. Gíslason, and H. Thorsteinsson. “Tackling the Challenge of H₂S Emissions” Proceedings, *World Geothermal Congress*, Melbourne, Australia (2015).
- [6] Hallsdóttir B.S., K. Harðardóttir, J. Guðmundsson, A. Snorrason, and J. Þórsson. “Emissions of greenhouse gases in Iceland from 1990 to 2008” Umhverfisstofnun, National Inventory Report (2010): UST-2020:05.
- [7] Stefánsson A., S. Arnórsson, I. Gunnarsson, H. Kaasalainen, and E. Gunnlaugsson. “The geochemistry and sequestration of H₂S into the geothermal system at Hellisheiði, Iceland” *Journal of Volcanology and Geothermal Research* 202 (2011): 179-188.
- [8] Gunnarsson I., B.M. Júlíusson, E.S.P. Aradóttir, B. Sigfússon, and M.Th. Arnarson. “Pilot Scale Geothermal Gas Separation, Hellisheiði Power Plant, Iceland” Proceedings, *World Geothermal Congress*, Melbourne, Australia (2015).
- [9] Gunnarsson I., E.S. Aradóttir, E.H. Oelkers, D.E. Clark, M.Th. Arnarsson, B. Sigfússon, S.Ó. Snæbjörnsdóttir, J.M. Matter, M. Stute, B.M. Júlíusson, and S.R. Gíslason. “Rapid and cost-effective capture and subsurface mineral storage of carbon and sulfur” *International Journal of Greenhouse Gas Control* (in press, pending minor revisions).
- [10] Franzson H. “Nesjavellir, Borholujardfraedi, Vatnsgengd i jardhitageymi (Nesjavellir, Borehole geology, Geothermal Fluid Type)” Orkustofnun (1988): OS-88046/JHD-09.
- [11] Franzson H., E. Gunnlaugsson, K. Árnason, K. Sæmundsson, B. Steingrímsson, and B. Harðarson. “Hengill geothermal system, conceptual model and thermal evolution” Proceedings, *World Geothermal Congress* (2010).
- [12] Snæbjörnsdóttir S.Ó. “The Geology and Hydrothermal Alteration at the Western Margin of the Hengill Volcanic System” University of Iceland, Master’s Thesis (2011).
- [13] Parkhurst D.L., and C.A.J. Appelo. “Description of input and examples for PHREEQC. Version 3-a computer program for speciation, batch-reaction, one-dimensional transport, and inverse geochemical calculations” *U.S. Geological Survey Techniques, Methods Report*, Book 6, chapter A43 (2013): 1-497.
- [14] Neveu M., S.J. Desch, and J.C. Bastillo-Rogez. “Aqueous geochemistry in icy world interiors: Equilibrium fluid, rock, and gas compositions, and fate of antifreezes and radionuclides” *Geochimica et Cosmochimica Acta* 212 (2017): 324-371.
- [15] Voigt M., C. Marieni, D.E. Clark, S.R. Gíslason, and E.H. Oelkers. “Evaluation and refinement of thermodynamic databases for mineral carbonation” *Energy Procedia* (2018): this issue.